Westerly Wind Bursts: ENSO's Tail Rather than the Dog?

IAN EISENMAN

Department of Earth and Planetary Sciences, Harvard University, Cambridge, Massachusetts

LISAN YU

Woods Hole Oceanographic Institution, Woods Hole, Massachusetts

ELI TZIPERMAN

Department of Earth and Planetary Sciences, and Division of Engineering and Applied Sciences, Harvard University, Cambridge, Massachusetts

ABSTRACT

Westerly wind bursts (WWBs) in the equatorial Pacific occur during the development of most El Niño events and are believed to be a major factor in ENSO's dynamics. Because of their short time scale, WWBs are normally considered part of a stochastic forcing of ENSO, completely external to the interannual ENSO variability. Recent observational studies, however, suggest that the occurrence and characteristics of WWBs may depend to some extent on the state of ENSO components, implying that WWBs, which force ENSO, are modulated by ENSO itself.

Satellite and in situ observations are used here to show that WWBs are significantly more likely to occur when the warm pool is extended eastward. Based on these observations, WWBs are added to an intermediate complexity coupled ocean–atmosphere ENSO model. The representation of WWBs is idealized such that their occurrence is modulated by the warm pool extent. The resulting model run is compared with a run in which the WWBs are stochastically applied. The modulation of WWBs by ENSO results in an enhancement of the slow frequency component of the WWBs. This causes the amplitude of ENSO events forced by modulated WWBs to be twice as large as the amplitude of ENSO events forced by stochastic WWBs with the same amplitude and average frequency. Based on this result, it is suggested that the modulation of WWBs by the equatorial Pacific SST is a critical element of ENSO's dynamics, and that WWBs should not be regarded as purely stochastic forcing. In the paradigm proposed here, WWBs are still an important aspect of ENSO's dynamics, but they are treated as being partially stochastic and partially affected by the large-scale ENSO dynamics, rather than being completely external to ENSO.

It is further shown that WWB modulation by the large-scale equatorial SST field is roughly equivalent to an increase in the ocean–atmosphere coupling strength, making the coupled equatorial Pacific effectively self-sustained.

1. Introduction

Westerly wind bursts (WWBs), defined roughly as westerly gusts in the equatorial Pacific with a strength of at least 7 m s^{-1} and duration of 5–20 days (cf. Harrison and Vecchi 1997), occur about 3 times per year on average with higher occurrence associated with El Niño events (Verbickas 1998). They have been linked to a variety of atmospheric phenomena including paired and individual tropical cyclones (Keen 1982), cold surges from midlatitudes (Chu 1988), the convectively active phase of the Madden–Julian oscillation (Chen et al. 1996; Zhang 1996), or a combination of all three (Yu and Rienecker 1998).

WWBs cause downwelling Kelvin waves, clearly observable in buoy data, that propagate eastward and are associated with warming (McPhaden et al. 1988). It therefore makes sense to expect that WWBs may be involved with the onset of El Niño events (Latif et al. 1988; Lengaigne et al. 2004; Luther et al. 1983; Perigaud and Cassou 2000). Indeed, WWBs have been observed

Corresponding author address: Ian Eisenman, Dept. of Earth and Planetary Sciences, Harvard University, Cambridge, MA 02138.
E-mail: eisenman@fas.harvard.edu

to occur in association with the onset of every significant El Niño event for the past 50 years (Kerr 1999; McPhaden 2004). Observational studies have demonstrated that sea surface temperature (SST) anomalies increase in response to WWBs (Vecchi and Harrison 2000) and that WWBs occur more frequently and energetically, and extend farther eastward, prior to and during El Niño events (Delcroix et al. 1993; Harrison and Vecchi 1997; McPhaden 1999; Vecchi and Harrison 2000; Verbickas 1998). In models, El Niño's first stochastic optimal (the spatial structure of surface ocean forcing that leads to the greatest interannual variability) has been suggested to resemble the structure of a WWB (Moore and Kleeman 1999), although this result appears to be largely model dependent (Blumenthal 1991; Fan et al. 2000; Moore and Kleeman 1996, 2001; Penland and Sardeshmukh 1995; Xue et al. 1997).

The role of WWBs in the dynamics of El Niño–Southern Oscillation (ENSO), while clearly important, remains elusive. Although the evidence described above strongly suggests their importance to ENSO, some reliable ENSO hindcasts have been obtained without including WWBs (e.g., Chen et al. 2004). Furthermore, the exceptionally large El Niño of 1997–98, whose occurrence and amplitude were not well predicted by most models (Barnston et al. 1999; Landsea and Knaff 2000), had an unusually high occurrence of WWBs (McPhaden 1999; Vecchi and Harrison 2000).

Because of their short time scale, WWBs are normally thought of as external to equatorial Pacific interannual variability and are thus treated in models as part of the stochastic forcing of ENSO. Stochastically forced ENSO models are typically either forced by noise that is effectively white in time and spatially projected directly onto the first stochastic optimal (e.g., Moore and Kleeman 1999), noise that is white in both time and space (e.g., Thompson and Battisti 2000), or noise with stationary statistics based on atmosphere and SST observations (e.g., Eckert and Latif 1997). Assuming that the stochastic forcing is stationary in time (or seasonally dependent) is equivalent to the assumption that the occurrence of WWBs does not depend on interannually varying ENSO components.

Recent observational studies, however, suggest that the occurrence of WWBs may depend to some extent on the state of the interannually varying ENSO components. Yu et al. (2003) used a blend of observations in a case study of several El Niño and La Niña events to suggest that WWBs are more prone to occur when the tropical Pacific warm pool, whose location is dominated by ENSO, is extended. Vecchi and Harrison (2000) found a highly significant relationship between warm central equatorial Pacific SST and the occurrence of

WWBs when the Niño-3 index (average eastern tropical Pacific SST) is close to normal. McPhaden (1999) observed that strong equatorial surface winds occurred only over areas with SST greater than 29°C and that WWBs seemed to migrate eastward in tandem with the 29° SST isotherm during the 1997–98 El Niño. All of these studies suggest that the occurrence and characteristics of WWBs may depend to some extent on the state of the interannually varying ENSO components.

The purpose of this paper is to demonstrate the effects on ENSO dynamics when WWBs are modulated by the large-scale SST in the equatorial Pacific, and hence by ENSO. Motivated by observations, we thus call into question the common practice of treating WWBs as a stochastic forcing in ENSO models. We argue that regarding WWBs not as external forcing, but rather as a forcing element whose occurrence and characteristics are modulated by the ENSO cycle, makes a very significant difference in the effect these events have on ENSO. Specifically, we find that WWB events modulated by the SST force an ENSO response twice as large as the response to the same average number of WWB events that are completely stochastic. We therefore conclude that it is critical to understand and account for the dependence of WWB events on the large-scale SST and hence ENSO.

The role of WWBs is also relevant to the issue of ENSO's irregularity. The two main hypothesized mechanisms to explain the irregularity are, first, stochastic forcing (Kessler 2002; Kleeman and Moore 1997; Moore and Kleeman 1996, 1999; Penland and Sardeshmukh 1995; Thompson and Battisti 2000) amplified by the nonnormal ENSO dynamics (Farrell 1988) and, second, deterministic low-order chaos (Chang et al. 1994; Jin et al. 1994; Tziperman et al. 1994, 1995). If WWBs are purely stochastic (i.e., additive noise), ENSO's irregularity may be due to this noise forcing. If they are regulated by the large-scale SST, however, the results can be quite different. We show here that when WWBs are determined by the SST their inclusion is roughly equivalent to an enhancement of the ocean–atmosphere coupling strength, which can lead to self-sustained ENSO events and even chaotic ENSO behavior driven by the deterministic WWBs and the seasonal cycle. In a sense (which we try to make more explicit below), one could think of WWBs as being multiplicative noise rather than additive noise. That is, the characteristics of the noise are random, but they still depend on the state of the system.

We discuss in this study the implications of our findings for the construction of ENSO models. A common procedure for dealing with the relation of the wind to the SST involves deriving a statistical atmospheric

model that represents the part of the wind stress that is linearly correlated with the SST, and then possibly adding a purely stochastic forcing on top of that. We attempt in the following to explain that this procedure may not be adequate should the WWBs indeed be modulated by the warm pool location and that the procedure would result in a biased representation of the effects of the WWBs.

It is worth emphasizing that this paper is not about a detailed realistic simulation of WWB events and their influence on ENSO. Rather, in the tradition of using conceptual models for understanding mechanisms of climate dynamics, we are including highly idealized WWBs in the Cane–Zebiak (CZ) coupled ocean–atmosphere model (Zebiak and Cane 1987) to contrast two extreme and likely unrealistic scenarios. In one, WWBs are completely stochastic and not affected by the large-scale SST. This is the way WWBs are typically modeled, but we argue that it disagrees with evidence from observations. The other scenario investigated here, extreme in the opposite direction, is one in which WWB events are modulated in a purely deterministic way by the large-scale SST (roughly, we impose WWBs whenever the warm pool is extended). We believe that the most realistic scenario lies somewhere in between these extreme cases. The purpose of this paper is to examine these asymptotic limits of the problem in order to shed light on the role of WWBs that have a stochastic element in their characteristics and occurrence but are affected by the structure of the large-scale SST. We emphasize that while we are proposing that WWB events are not to be treated as a purely external stochastic forcing of ENSO, we are still suggesting that they are an essential component of the ENSO system.

In section 2, we describe observational evidence that WWBs are modulated by ENSO. This is followed by a description of the model (Zebiak and Cane 1987) and some technicalities of parameterizing the modulation of WWBs by ENSO (section 3). Experiments in which WWBs are prescribed to be either modulated by the large-scale SST or purely stochastic are described and compared in section 4. We discuss the implications of our proposed paradigm for the role of WWB events to the construction of statistical atmospheric models, and to the issue of whether ENSO responds linearly or nonlinearly to WWBs, in section 5. We conclude in section 6.

2. Observational evidence of WWB modulation by ENSO

The increased occurrence of WWBs prior to and during most El Niño events has been observed and noted in the past (e.g., Delcroix et al. 1993; Keen 1982; Luther
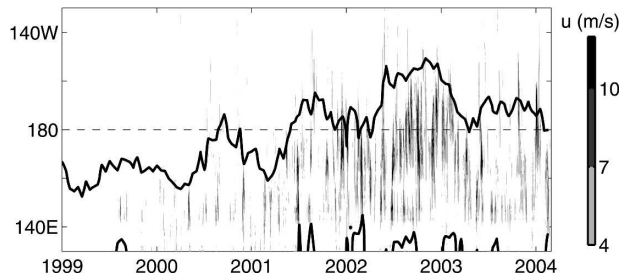

FIG. 1. Evidence for the modulation of WWBs by warm pool extension in high-resolution satellite data. Equatorial westerly wind anomalies $u_{anom} \geq 4$ m s^{-1} (shading) from QuikSCAT superimposed on warm pool extension (contour line) as measured by the 29°C total SST isotherm from TMI. The dashed line marks the date line. WWBs (patches of dark shading in figure; see discussion of the spectrum of WWB definitions in section 2) appear to occur more frequently when the warm pool is extended.

et al. 1983; Vecchi and Harrison 2000; Verbickas 1998). We begin here with an analysis of high-resolution satellite observations suggesting that WWBs are indeed affected by ENSO. We show that their time of occurrence, longitudinal extent, location, and amplitude appear to be modulated by the warm pool extension. The satellite data, however, spans only a fairly short time period. For this reason, we turn to longer running in situ buoy measurements from the tropical Pacific, which do not resolve WWBs as fully but allow us to make rough quantitative estimates of the dependence of WWB occurrence on the warm pool. The discussion of observations in this section motivates our modeling experiments presented below.

Consider first Fig. 1, which shows the location of WWBs superimposed on the warm pool as measured by the region with SST greater than 29°C. Winds are retrieved from the SeaWinds scatterometer onboard the Quick Scatterometer (QuikSCAT) satellite, and SST measurements are from the Tropical Rainfall Measuring Mission (TRMM) Microwave Imager (TMI). The two datasets are daily products with spatial resolution of 0.25° by 0.25°. The winds were smoothed with a 3-day running mean, and the SST was smoothed onto a 15-day grid. It is clear from this figure that most WWBs occur when the warm pool is extended. The events happen preferentially during El Niño years and are clustered into groups of consecutive bursts. Note that the zonal extent of WWBs also appears to be larger when the warm pool is extended. Using a somewhat different isotherm as a measure for the warm pool extent leaves this picture qualitatively unchanged.

The correlation between warm pool displacement and the easternmost longitude of 5 m s^{-1} westerly wind is presented in Fig. 2. The correlation coefficient is 0.62 based on 778 pairs.
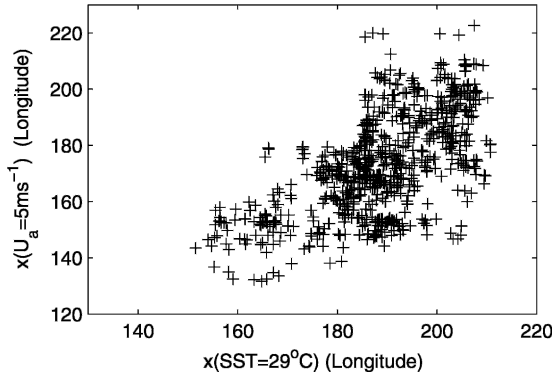
FIG. 2. Scatterplot of the warm pool displacement (measured by the location of the 29°C equatorial SST isotherm) vs the eastern-most longitude of westerly winds at the equator with amplitude greater than 5 m s^{-1} for the period from Aug 1999 to Feb 2004. The correlation between the two is 0.62. This figure implies that the eastern edge of a WWB typically migrates zonally above the edge of the warm pool.

Figure 3 demonstrates that strong westerly gusts that are typical of WWBs occur preferentially over regions with SST greater than 29°C, again demonstrating the strong link between WWBs and the warm pool location. These findings motivate our hypothesis that WWBs are strongly modulated by the warm pool location and therefore by the large-scale ENSO dynamics rather than being a completely external stochastic forcing.

To further motivate the modeling study, we also examine the longer-running but lower-resolution wind
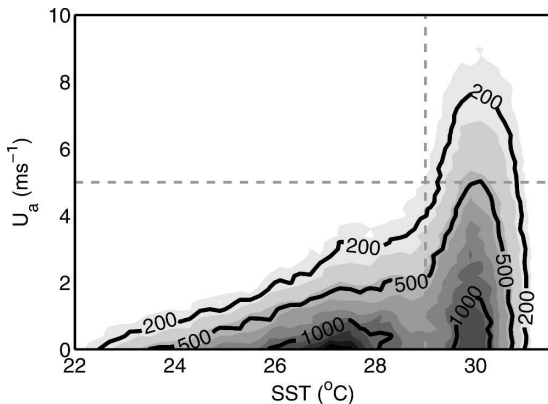

FIG. 3. Number of westerly wind observations as a function of the SST above which they occur and wind speed anomaly. The SST and zonal wind are averaged over the equatorial band (5°S, 5°N) and grouped into 0.2°C and 0.2 m s^{-1} bins. The contour lines indicate the number of events per bin. Dashed lines represent 5 m s^{-1} and 29°C; note that events with wind speed in excess of 5 m s^{-1} (roughly, WWBs; see discussion of the spectrum of WWB definitions in section 2) occur exclusively over warm water.

and SST data from the in situ Tropical Atmosphere Ocean array (TAO) buoy array measurements (Mc-Phaden et al. 1998). Although some TAO data are available back to 1980, the data in the central and western equatorial Pacific are very sparse before around 1990. We construct a 14-yr (1990–2004) daily time series of equatorial zonal wind and SST by averaging available buoy measurements between 2°S and 2°N. We subtract the seasonal cycle from the winds to compute wind anomalies, interpolate (concurrently in space and time) over periods with missing data, and smooth both datasets with a 5-day running mean.

Next, we crudely define WWBs as an incident of anomalous westerly wind greater than 7 m s^{-1} within a period of 5 or more days of westerly wind greater than 4 m s^{-1}. The separation between consecutive events is defined by requiring that the wind drop to 2 m s^{-1} below its peak value during a WWB before the next WWB can begin. The SST and anomalous wind data are plotted in Fig. 4. WWBs, as defined above, are indicated by black dots below the horizontal axis.

Using this scheme, we find an average of 3.1 WWBs per year. These WWBs typically have peak zonal wind velocities in the range of 7–13 m s^{-1} and last around 10 days. The increased occurrence of WWBs when the warm pool is extended is clear from this analysis. The 29° isotherm extends past the date line 55% of the time, but 77% of WWBs occur when it is extended. By application of Bayes' theorem, this implies that WWBs are 2.8 times more likely to occur when the warm pool is extended. We also note that most WWBs occur during the boreal winter and spring, with significantly less occurring during the boreal summer; only 9% of the WWBs occur during the July–September quarter (the average percent of WWBs in the other three quarters is 30%).

The scheme used here to identify WWBs is part of a spectrum of possible WWB definitions. This definition was chosen because we are interested in WWBs that are related to the warm pool location and are likely to play a significant role in triggering El Niño events. It is similar to the definition in Verbickas (1998), who identified WWBs as anomalous winds in the equatorial Pacific just west of the date line greater than 5 m s^{-1} for 2–39 days. She found 3.8 WWBs per year on average, occurring most frequently between November and April. It is not surprising that she found slightly more WWBs than we do since she included briefer bursts in her analysis. In contrast to this, Harrison and Vecchi (1997) classified WWBs based on their location. They considered eight regions in the tropical Pacific and called a WWB an incident in which the area-averaged anomalous wind in any region is greater than 2 m s^{-1}
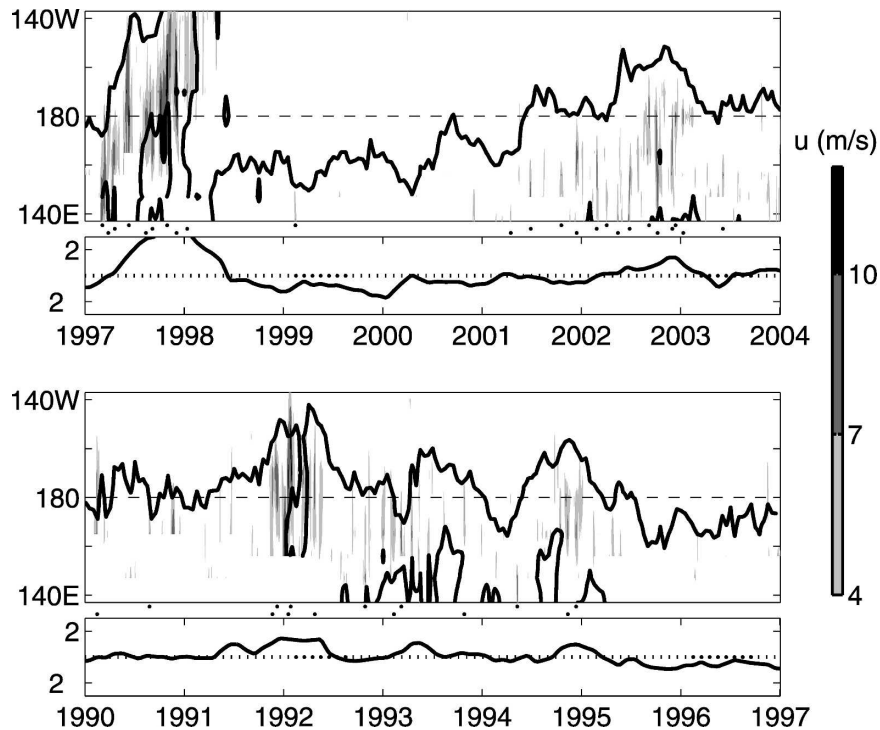
FIG. 4. Evidence for WWB modulation by warm pool extension in the TAO buoy data. Equatorial wind anomalies $u_{\mathrm{anom}} > 4$ m s^{-1} (shading) superimposed on warm pool extension (contour line) as measured by the 29°C total SST isotherm. Similar to Fig. 1, except that this dataset extends longer and has far lower spatial resolution. WWBs, as defined in the text, are indicated by black dots below the horizontal axis. The dots are staggered vertically to aid in counting. As described in the text, these data imply that WWBs are 2.8 times more likely to occur when the warm pool is extended. A time series of observed Niño-3 SST anomalies from the seasonal cycle, from the NOAA/NCEP Climate Prediction Center, is plotted below each contour plot.

for at least 3 days. Our WWBs are most similar to their type C, except that their scheme includes far weaker events. They find 6.3 such weaker type C WWBs per year on average. When they consider only strong WWBs, their type C WWBs display a seasonal bias in which there is a higher occurrence during boreal winter, similar to what we find in the TAO data and apply in the simulations below.

Although WWBs are typically defined using wind anomalies from the seasonal cycle, as we have done above, one might argue that it would be more fair to subtract the ENSO cycle from the wind field before identifying WWBs. Since the winds display strong ENSO-related interannual variability, if WWBs are superimposed on this with stationary statistics, an identification scheme based on the wind anomaly field would still find more WWBs during El Niño years since the annually averaged winds are more westerly. We address this issue briefly here. We high-pass filter the wind anomaly field to eliminate variability on time scales longer than one year and then use the identifi-

cation scheme described above to find WWBs. This leads to the identification of 1.9 WWBs per year, with 69% of them occurring when the warm pool is extended, implying that WWBs are 1.8 times more likely to occur when the warm pool is extended (the SST data is not filtered). In this scheme, no WWBs occur during July–September.

We note that one cannot determine based on the above observations alone whether the extended warm pool is causing there to be more WWBs or whether the WWBs are occurring independent of the SST but enhancing ENSO and moving the warm pool east. This issue was addressed by Yu et al. (2003), who suggested that ENSO in fact modulates WWB events via the extended warm pool, which causes the western equatorial east–west sea level pressure gradient to increase. The increased pressure gradient then enhances equatorial cyclonic circulation, which allows the penetration of cold surges from midlatitudes to the equatorial Pacific region, and hence contributes to prolonged WWB events. This strengthening and eastward shift of WWBs

during the developing stage of El Niño may also be related to changes in cloud radiative forcing (Bergman and Hendon 2000). If the WWBs and the large-scale warm pool structure are coupled, one does not expect to be able to differentiate cause and effect in the observations.

Based on this analysis, we now proceed to model experiments using an intermediate complexity coupled ocean–atmosphere model that we force with WWBs. We examine two extreme scenarios. In the first, WWBs are modulated in a completely deterministic way by the warm pool location. In the second, they are completely stochastic. The second scenario is similar to the way WWBs are typically treated in ENSO models that do not resolve the WWBs explicitly (i.e., in intermediate complexity ENSO models, hybrid coupled models, and other models that do not include an atmospheric GCM). We suggest that the most realistic situation would lie somewhere in between the two scenarios discussed here, that is, that WWBs should be treated stochastically but that their probability of occurrence and characteristics should be a function of the warm pool location. This implies that WWBs should be treated as similar to multiplicative rather than additive noise, as discussed in more detail below.

3. Modulated WWBs in the CZ coupled model

The model experiments are conducted using the CZ intermediate complexity coupled ocean–atmosphere model (Zebiak and Cane 1987), a nonlinear model of anomalies from the seasonal cycle in the tropical Pacific. The CZ ocean equations are solved by integrating for the ocean Kelvin and Rossby waves separately and then solving the ocean SST equation with a 10-day time step. At each 10-day time step, a Gill-like atmospheric model is used to force the ocean with anomalous winds in quasi steady state with the SST. The atmospheric model, in turn, is driven by heating that is a function of the local SST and the large-scale moisture convergence.

To carry out the model experiments described below using the CZ model, we need to change the model in two ways. First, we reduce the ocean–atmosphere coupling coefficient in order to stabilize the model. Once stabilized, an initial perturbation to the model leads to variability that eventually decays. In this stable (or damped) regime, some forcing such as WWBs is needed to excite ENSO events. This is the regime in which most studies of stochastic forcing of ENSO have been carried out. The second change involves the parameterization of WWBs in the model as a function of the warm pool extension (i.e., SST distribution). These two changes are described in more detail in the following two subsections.

a. Stabilizing the CZ model

We stabilize the model by reducing the coupled ocean–atmosphere ENSO instability. The winds force the currents in CZ using a standard bulk formula,

$$\tau = \rho_{\text{air}} C_d |\mathbf{u}| \mathbf{u},$$

where τ is wind stress, ρ_{air} is the density of air, C_d is the drag coefficient, and $\mathbf{u}$ is the surface wind velocity. The drag coefficient may be regarded as a parameter governing the overall ocean–atmosphere coupling in the CZ model (Cane et al. 1990). We varied it according to

$$C_d = \text{R}^* C_{\text{cz}},$$

with C_{cz} the value used in CZ. When R^* is reduced below 0.795, the coupled instability in the model is eliminated and the model becomes stable. We used $R^* = 0.78$, sufficiently below the stability threshold.

b. Parameterizing WWB modulation by warm pool extension

We added perturbations resembling WWBs to the model wind stress field. The WWBs have Gaussian structure in longitude and latitude with meridional and zonal extent of 6° and 20°, respectively, and are centered on the equator at 175°E. This spatial structure is similar to the composite of WWB observations in Harrison and Vecchi (1997) for what they call type C WWBs (the type of WWBs which appears to be most likely to trigger an El Niño event, as well as the most common category of WWB according to their analysis). The amplitude of the WWBs is 1.7 dyn cm^{-2}, a stress approximately equivalent to a maximum wind speed of 10 m s^{-1} (consistent with section 2). The space and time scales of observed *easterly* wind anomalies are typically much larger, and the amplitudes much smaller, than WWBs (Harrison and Vecchi 1997). Motivated by this lack of observed easterly wind bursts, we added only westerly wind perturbations to the model.

The modulation of the WWBs is carried out using the location of the edge of the warm pool. At each 10-day time step of the model between the months of October and June, a WWB is triggered if the 28.7°C equatorial SST isotherm extends east of the date line. A range of isotherm values that are approximately consistent with observations were considered, and this one was chosen as a best fit to observed characteristics in the resulting simulation. Each time a WWB is triggered, it blows steadily for 20 days followed by a 40-day lull during which no WWB can occur. This 40-day minimum separation is in rough agreement with observations (Figs. 1 and 4). The qualitative results of this study are not sensitive to modest changes in the parameters used for the WWB parameterization, including doubling or

eliminating the lull period. These parameterizations are motivated by the discussion in section 2, as well as the observations in Harrison and Vecchi (1997).

The 20-day WWB duration is on the long side of observed events, but it is required by our model time step of 10 days. Using events that last a single time step may lead to numerical problems, so we are constrained to use an event that is two time steps long. A study using models that allow for shorter time scales would clearly be needed to examine the sensitivity to the length of the WWB events.

Note that the WWB events used here are meant to represent the episodic WWBs with a duration of a week or two in the observed record, rather than the intraseasonal scale wind perturbations such as those due to the Madden–Julian oscillation (MJO) whose interactions with ENSO have been studied fairly extensively (e.g., Bergman et al. 2001; Kessler 2001; Kessler et al. 1995; Zavala-Garay et al. 2005). The effects of the MJO on the CZ model were also studied by Zebiak (1989), who found that weak stochastic forcing with power mostly in the 20–60-day band had little effect on model simulations and hindcasts. This weak response may have resulted from the model being in its standard unstable regime, making the coupled dynamics dominate the stochastic forcing. Our results also suggest that the response would have been stronger if the stochastic forcing depended on the SST.

In these experiments, the modulation of WWBs by the warm pool is idealized compared to the observations discussed in section 2 mainly in two ways. First, only the timing of the events is controlled by the warm pool location; the duration, fetch, and other characteristics are fixed in the model. Second, in the modulated WWB experiments we eliminate any stochastic element from the WWB dynamics and make the WWB timing completely determined by the SST; WWBs always occur when the warm pool is extended and hence force every El Niño event. While these are clearly extreme simplifications of the above observational analysis, they help demonstrate the dynamical effects of WWB modulation by ENSO in the simplest possible scenarios.

4. Dynamical consequences of WWB modulation by the SST

We begin by comparing runs of the CZ model in which the timing of the WWBs is determined (modulated) by the warm pool location with model experiments in which WWBs are specified as a purely stochastic forcing (section 4a). Next, we apply various bandpass filtering to the forcing and output of these runs in order to understand the results (section 4b), and

we demonstrate that the effect of WWB modulation on the amplitude of ENSO is very significant. Finally (section 4c), we show that the introduction of modulated WWBs is roughly equivalent to increasing the coupling between the ocean and the atmosphere, and we discuss the implications of this result to the issue of ENSO being self-sustained versus damped and the issue of stochastically driven ENSO irregularity versus low-order chaos in the equatorial Pacific.

a. Modulated versus stochastic WWBs

Introducing WWBs that are modulated by the warm pool location as described in section 3b, we find that the stabilized CZ model now displays sustained ENSO variability (Fig. 5b) of a similar amplitude to the CZ standard run (Fig. 5a). The modulated WWBs produced by the model tend to be clustered (Fig. 5b) very similarly to the way this happens in the observations (Figs. 1 and 4). Note that the modulated WWB run (Fig. 5b) is characterized by irregular ENSO events although there is no element of stochasticity in this run. We will return to this issue in section 4c.

To determine the magnitude of the effect of WWB modulation by ENSO, we replace the WWB trigger in the modulated WWB simulation with a stochastic trigger, leaving everything else unchanged. WWBs are still forbidden during the summer months and last 20 days followed by a 40-day lull, but the triggering is computed stochastically with the probability of triggering at each time step adjusted such that the average number of WWBs each year matches the modulated WWB run. The result, shown in Fig. 5c, is that the stochastic run has about half the ENSO variability of the modulated WWB run shown in Fig. 5b. More quantitatively, the Niño-3 standard deviation of the stochastic run, calculated from model years 200–1200 (the integration starts with a perturbation during year 0), is only 58% that of the modulated run. Repeating this comparison while varying the SST isotherm used for triggering WWBs as well as the WWB amplitude within physically reasonable ranges leads to similar Niño-3 standard deviation ratios. Similarly, this ratio is not very sensitive to the coupling strength parameter R^*. Raising or lowering R^* by some 10% while remaining below the stability threshold ($R^* = 0.795$) does not significantly affect these results. The implication of this result is that the correct inclusion of WWB modulation in ENSO models may be crucially important.

b. Understanding the different response to modulated and stochastic WWBs

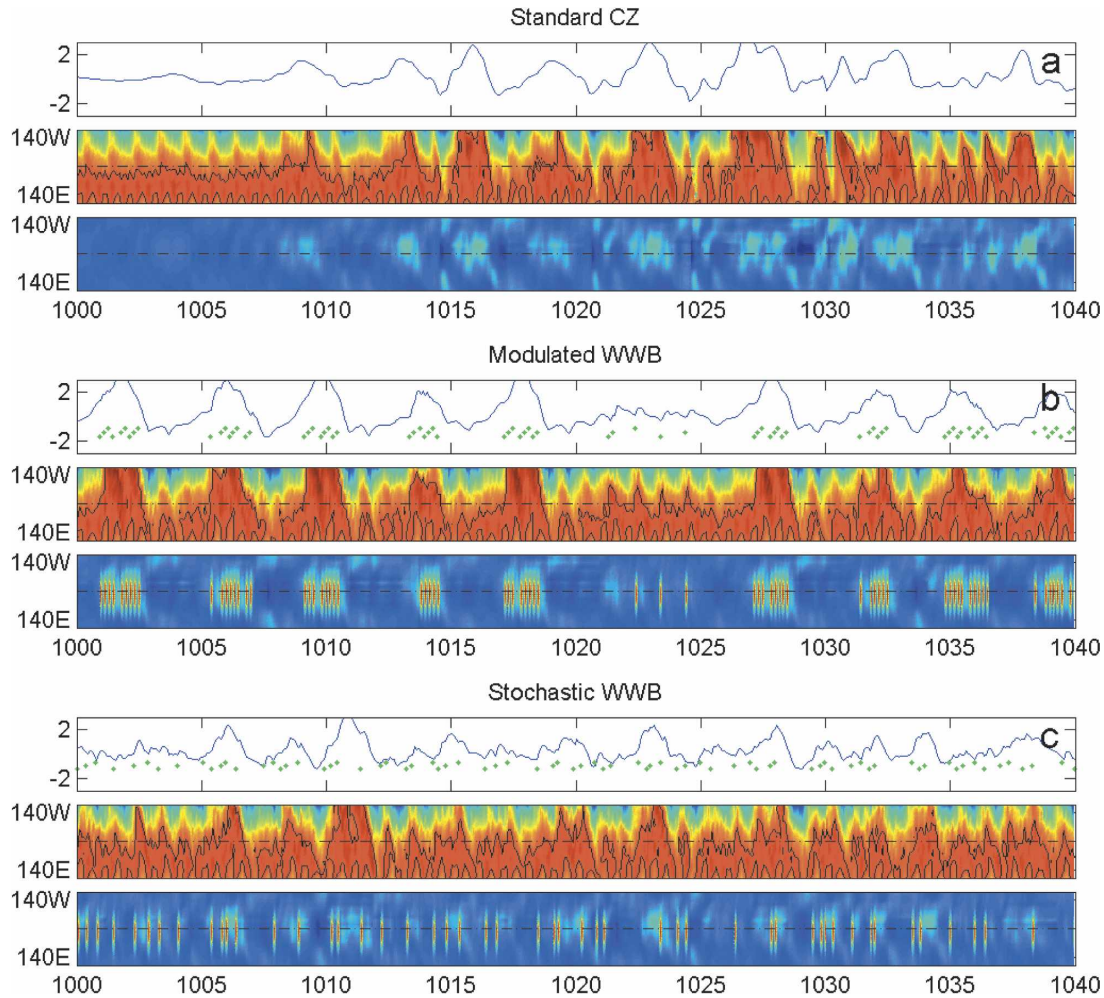While the above difference in the rms variability between the stochastic WWB runs and the modulated

FIG. 5. Model integrations with no WWBs, modulated WWBs, and stochastic WWBs. (a) The CZ standard run ($R^* = 1$). The standard deviation for this run is std dev(Niño-3) = 1.1°C. (b) Reduced coupling ($R^* = 0.78$) with imposed WWBs that are modulated by the ENSO state. The modulation results in 1.9 WWBs per year on average, and std dev(Niño-3) = 1.4°C. Details of the WWB parameterization are described in section 3b. (c) Reduced coupling ($R^* = 0.78$) with imposed stochastic WWBs such that there are 1.9 WWBs per year on average: Std dev(Niño-3) = 0.78°C. In each of the three panels, the model Niño-3 time series is plotted above longitude–time contours of equatorial total SST and zonal wind stress anomaly for model years 1000–1040. Green dots below the Niño-3 curve indicate WWBs (the dots are staggered vertically to aid counting). The contour plot ranges are 23°–30°C for SST and −0.5 to 2 dyn cm^{-2} for wind stress. The 28.7°C isotherm, used for WWB triggering as described in the text, is indicated by a solid black line. A dashed black line marks the date line in both contour plots.

WWB runs is quite compelling, it is, in fact, an underestimate. Much of the variance in the stochastic WWB run (Fig. 5c) is due to short time-scale variability that has nothing to do with ENSO. To isolate and quantify the actual effects of the WWB modulation on ENSO events, we now analyze several runs in which the forcing has been first modified with a low-pass filter.

We begin by running the model with modulated and stochastic WWB events, as shown in Figs. 5b,c, and saving the WWB forcing signal. We then low-pass filter the forcing to preserve only frequencies slower than

one year (note that even though WWBs occur episodically on a time scale of weeks, there are more in some years than others, so the WWB time series has energy in the interannual band). Finally, we rerun the stabilized model imposing the filtered WWB forcing from the modulated and then stochastic WWB runs [similar to the experiments of Roulston and Neelin (2000)]. Note that in these experiments, the filtered modulated run is not actually controlled by the SST distribution in the current run. Rather, it has been controlled by the SST distribution in the original unfiltered modulated
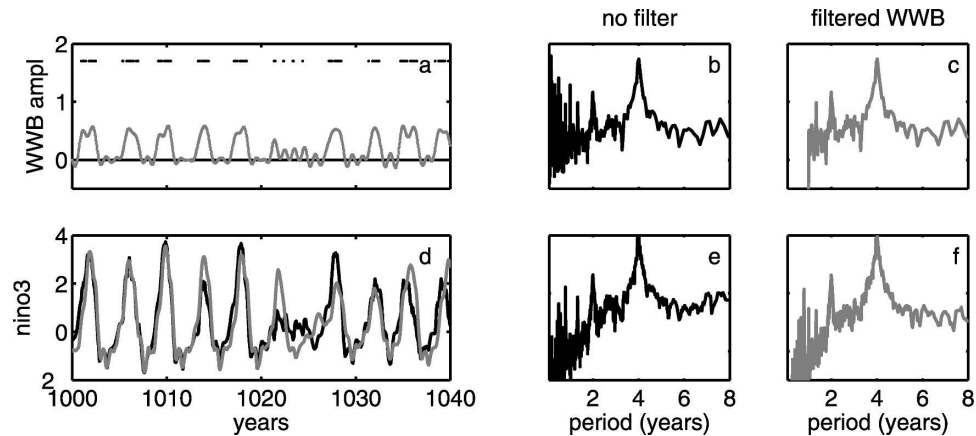
FIG. 6. Modulated WWB events with and without a 1-yr low-pass filter on the WWB forcing. The black curves represent the original (unfiltered) run. The gray curves represent the runs in which the WWB forcing was saved, low-pass filtered, and then a new experiment was run in which this filtered forcing was imposed. The WWB amplitude time series is plotted for both runs (a) next to the WWB power spectrum for the (b) unfiltered and (c) filtered WWB simulations. (d) The Niño-3 time series and (e), (f) spectra are plotted for both runs in the lower panel. In the unfiltered run (black), the WWB amplitude is either 0 (off) or 1.7 (on) at each time step. We filtered out the fast variability from the WWB forcing, and the new WWB time series is superimposed (gray). All power spectra are computed from model years 200–1200 using the Thompson multitaper method. Spectral density is plotted in arbitrary logarithmic units that span 5 decades and are consistent between adjacent plots.

WWB run, and after filtering it is imposed as a specified external forcing in this run. The results are shown in Figs. 6 and 7. It can be seen clearly that the filtering of the forcing in the modulated WWB case has a fairly small effect on the amplitude of the ENSO variability in the model, but that it eliminates much of the variability in the stochastic WWB case.

Figure 8 summarizes a range of model experiments with filtered WWB forcing. The solid and dashed curves show the ENSO variability in the modulated

WWB and stochastic WWB experiments, respectively, as a function of the cutoff of a low-pass filter applied to the WWB forcing. ENSO variability is measured here as the Niño-3 standard deviation after a 2–8-yr bandpass filter is applied to the Niño-3 time series to isolate variability associated with ENSO. At a filtering of two years, the ratio of the 2–8-yr bandpass Niño-3 standard deviation between modulated and stochastic WWB experiments is $1.3°–0.43°C$, a difference of about a factor of 3 in the ENSO response to WWB forcing.
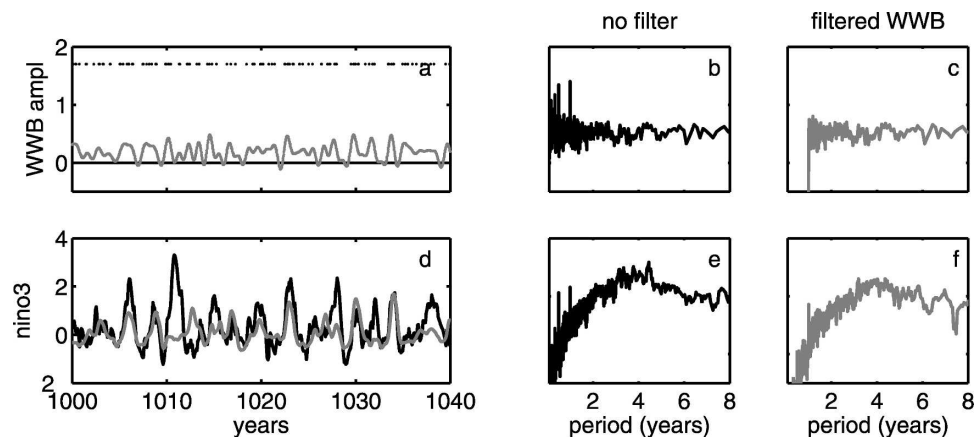

FIG. 7. Stochastic WWB events, with the average WWB frequency identical to the modulated run (Fig. 6), with (black) and without (gray) a 1-yr low-pass filter on the WWB forcing. See description of plots in Fig. 6. Note that the spectral densities plotted in this figure are consistent between adjacent plots but differ from the ranges plotted in Fig. 6.
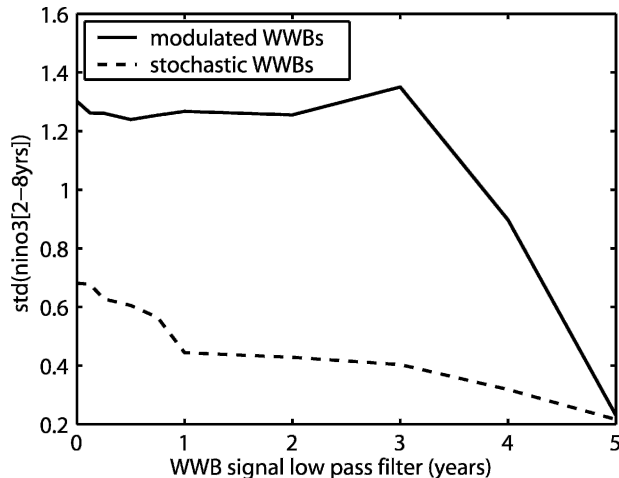
FIG. 8. ENSO response as a function of the cutoff of the low-pass filter applied to the WWB forcing. The vertical axis is standard deviation of the Niño-3 time series after a 2–8-yr bandpass filter is applied to isolate the Niño-3 variability associated with ENSO. The horizontal axis is cut off of the low-pass filter applied to the WWB forcing applied to the model. Solid line is for modulated WWB events and dashed line is for the stochastic WWB run. In both cases, the WWB time series is extracted from the model run (Figs. 5b,c), filtered, and then applied to the stabilized CZ model (Figs. 6 and 7). A point in this figure at 2 yr, e.g., is the standard deviation of the 2–8-yr Niño-3 bandpass when the CZ model is run with the WWB forcing filtered to eliminate variability faster than 2 yr. Note that in the modulated case (solid line), eliminating the rapid variability in the forcing does not change the Niño-3 response significantly, implying that ENSO is responding to (i.e., resonating with) the slow component of the WWBs (cf. Roulston and Neelin 2000).

The novel and interesting aspect in this analysis is that we propose that the forcing in the modulated WWB case has a strong low-frequency component due to the interaction of the WWB events and the large-scale SST field. The forcing in the purely stochastic case has less power at low frequencies and more at high frequencies. Thus the role of the feedback between WWBs and ENSO is mainly to amplify the power of the WWB signal in the interannual band. When the feedback is eliminated but the low-frequency amplification is maintained, the spectral properties of the model response are virtually unaltered (Figs. 6b,c).

This analysis indicates that the model variability in the modulated WWB case (solid curve in Fig. 8) is mostly a linear response to the forcing, consistent with the point of view of Roulston and Neelin (2000), who showed that an intermediate complexity coupled model similar to CZ responded mainly to the slow component of stochastic noise forcing, and Zavala-Garay et al. (2005), who used an intermediate complexity model and found that ENSO responds linearly to the low-

frequency power of the MJO. In the stochastic WWB case, however, the WWB energy is far less peaked in the interannual band, and the model appears to be responding nonlinearly to the forcing, rectifying fast WWB variability into slow ENSO amplitude. This is seen by the reduction in variance shown by the dash in Fig. 8 for WWB filtering with a cutoff shorter than one year, which implies that WWB forcing on time scales faster than one year affects the variance of Niño-3 on time scales of 2–8 yr. This appears to agree with the results of Kessler and Kleeman (2000), who, in contrast to Roulston and Neelin (2000), found that an ocean GCM forced by climatological winds responded to a purely sinusoidal MJO wind perturbation (60-day period) with gradual SST warming over the course of one year, implying a nonlinear response (i.e., slow response to fast forcing). Similarly, Boulanger et al. (2001) found that the response of an ocean GCM to WWB forcing at the onset of the 1997–98 El Niño was significantly nonlinear because of the interaction between the surface jet and thermodynamical fronts at the eastern edge of the warm pool. Thus our results appear to suggest that the CZ model is able to nonlinearly rectify variability faster than the interannual band into the ENSO cycle only when the amplitude of this variability is high. In the modulated WWB case, in which the total time-integrated energy is identical to the stochastic WWB case, it appears that not enough energy is varying rapidly to force a significantly nonlinear response.

The importance of the timing of WWB events has been investigated, for example, by Fedorov (2002) and Fedorov et al. (2003), who looked at the energetics of ENSO and showed that, when WWBs occur about 6 months before a warm event, they are most efficient for strengthening El Niño. Since warm pool extension leads Niño-3, this is roughly when WWBs begin to occur in the modulated WWB model.

c. On the equivalence of WWBs and ocean–atmosphere coupling strength

In the modulated WWB run, WWB triggering is a function of the warm pool extension, which varies interannually between El Niño and La Niña episodes nearly in phase with the slackening and strengthening of the trade winds (changes in the trade winds slightly lag the warm pool extension). Thus we might expect the introduction of modulated WWBs to be similar to an enhancement of the interannual wind variability or equivalently the wind–current coupling strength (R^*). To probe this analogy, we integrated two hundred, seventy-two 1200-yr simulations with a variety of coupling strengths and WWB amplitudes. In each run, the model
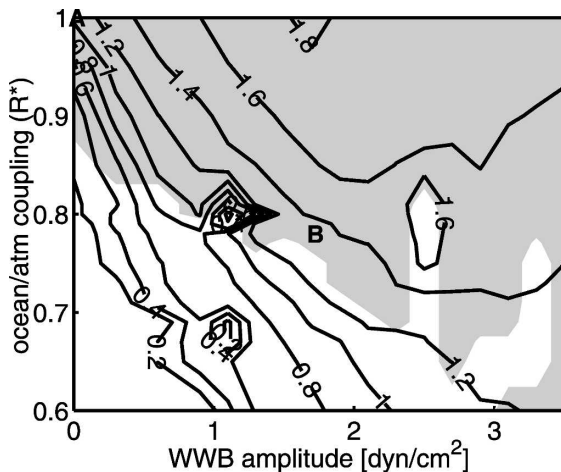
FIG. 9. Approximate equivalence between coupling strength and deterministic WWB amplitude. Shown is a contour plot of the standard deviations of Niño-3 from 272 modulated WWB model runs varying coupling strength $R*$ (vertical axis) and WWB amplitude (horizontal axis). Shading indicates the region in parameter space where ENSO variability is irregular and seemingly chaotic. The CZ standard run is marked **A,** and the modulated WWB run introduced in section 3 is marked **B.** Note the similarity between moving up and to the right in this plot in terms of both Niño-3 standard deviation and the threshold to chaos. A complete equivalence between the coupling strength and the WWB amplitude would result in the contours being straight lines from the bottom right to the top left of the figure. The equivalence is only approximate, however, as indicated by the irregular contour lines, including the "bull's-eye" features, and the unshaded fingers extending into the shaded chaotic region.

is spun up for 200 years after an initial perturbation and the following 1000 years are used for the analysis.

Figure 9 shows the Niño-3 standard deviation as a function of the coupling strength and WWB amplitude in these runs. The standard CZ model regime is at the top left in this figure (marked **A**), where the coupling strength is $R* = 1$ and the WWB amplitude vanishes. Note how the amplitude of ENSO variability increases with both the coupling strength and WWB amplitude. This indicates a rough equivalence between the coupling strength and the amplitude of WWB events modulated by the SST.

The figure also shows as a shaded area the parameter regime characterized by irregular, seemingly chaotic, runs (all runs in this figure are completely deterministic). While this is clearly an idealization, it demonstrates that the WWBs may induce a stronger effective ocean–atmosphere coupling and lead the coupled equatorial Pacific into a chaotic regime, as also occurs when the coupling strength itself is increased. The transition into an irregular ENSO regime occurs as we move away from the stable regime (bottom left of contour plot, where both the coupling strength and the WWB ampli-

tude are small) by increasing the coupling parameter (moving up along the left side). Starting from the same lower left point in parameter space, introducing WWBs and increasing their amplitude (moving to the right along the bottom) demonstrates qualitatively similar behavior. Both of these routes from the stable point in the lower left corner display a transition to chaos that is consistent with the quasi-periodicity route to chaos (Tziperman et al. 1995), showing stable, mode-locked, and then chaotic regimes.

This implies that as far as ENSO stability, amplitude, and irregularity are concerned, introducing modulated WWBs is roughly equivalent to increasing the air–sea coupling strength. Given that WWBs are normally seen as the proof that ENSO is stochastically driven, we feel that these results present WWBs in quite a different light.

We should comment, however, that this equivalence of WWB amplitude and coupling strength is only a very rough qualitative one. It holds in the sense demonstrated by Fig. 9, but not for some other circumstances for which a coupling strength may be defined and used, such as the direction of SST anomaly propagation. The onset of chaos is one example in which the equivalence is rough at best. Note that the transition between the shaded (chaotic) and unshaded (nonchaotic) regimes in Fig. 9 does not coincide with the contours of rms Niño-3 amplitude. We therefore emphasize that this equivalence cannot be used for any quantitative comparisons between the sensitivity to the coupling coefficient and the WWB amplitude.

Furthermore, note that while the overall structure of Fig. 9 is consistent with such an equivalence, there are some "bull's eye" features in the contour, as well as fingers of regular behavior extending into the chaotic region, at which this equivalence breaks down. Given the complex dependence of the CZ model on its parameters, with the interleaved regions of chaos, phase locking, and stable behavior, one does not expect a smooth dependence on any parameter, nor a perfect equivalence between WWB amplitude and coupling strength at all points in parameter space.

Because modulated WWB events occur only when the warm pool is extended, one may think about their effect as an enhancement of the ocean–atmosphere coupling coefficient only when the warm pool is extended, while leaving it unchanged otherwise. Perhaps this explains the quantitative differences between the enhancement of the coupling coefficient and the WWB modulation, which are discussed above.

Some aspects of the proposed equivalence shown in Fig. 9 between the coupling strength and the WWB amplitude may hold for purely stochastic WWB events

as well, and may be independent of the modulation effect that is the focus of this paper.

Finally, note that the modulated WWB run introduced in section 3 lies at (0.78, 1.7), marked **B** in Fig. 9. Thus we see that the parameters are fairly near to the chaotic threshold, which explains the low level of irregularity in the run and the somewhat sharp peak at 4 yr in the spectrum (Fig. 6b).

5. Discussion

a. Implications for the construction of statistical atmospheric models

We turn now to the implications of the above findings to the representation of WWB events in models that cannot resolve them. The discussion focuses on hybrid ENSO models (an ocean general circulation model coupled to a statistical atmosphere), but the ideas here can similarly be applied to any model that does not directly simulate WWBs. Statistical atmospheric models divide the wind into two components. One is a deterministic part that is linearly correlated with the SST, and the other is a stochastic part that is typically either ignored or included as an additive noise. The point we wish to make here is that, should the WWBs indeed be partially modulated by the SST, the division of the wind into these two components becomes inadequate.

To understand why this is the case, consider the following scenario. Suppose we have a record of SST and wind for a certain number of years. This will include El Niño years and La Niña years. Now, a statistical atmospheric model can be derived based on the sensitivity of the wind stress to SST anomalies. Such a statistical model is typically derived separately for each month and is based on the averaged sensitivity of the wind to SST anomalies during El Niño as well as La Niña years. We have made the case above (section 2), however, that WWB events tend to happen more frequently and with stronger amplitude and larger zonal extent during the onset of El Niño events. These WWBs are therefore at least partially correlated with the large-scale SST and would influence the wind sensitivity to the SST as represented by the statistical atmospheric model during the months in which El Niño develops.

This standard method results in a biased representation of the effects of the WWBs. The enhanced sensitivity of the wind to the SST is represented by the statistical atmospheric model for the appropriate months. During a simulation of the ENSO cycle, the enhanced sensitivity will influence both developing El Niño events and developing La Niña events. This enhanced sensitivity of the wind field to the SST, however, is typically obtained from an average over both El Niño years with many WWBs and La Niña years with few or none. Thus the statistical atmospheric model is expected to result in a sensitivity that is too weak during El Niño development and too strong during La Niña development.

The solution to this problem is, at least in principle, quite simple. One needs first to derive the statistical atmospheric model without the effects of the WWB events. This may be carried out by filtering these events out of the wind record before deriving the statistical atmospheric model. Next, it is necessary to identify the relation between the statistics of the WWBs and the large-scale SST (e.g., warm pool extent). This is not a simple task due to the shortness of the available high-resolution record, but Figs. 1 and 4 indicate that some rough estimate of the WWB–SST relation may be obtained. The final step that we suggest would be to run the statistical atmosphere and add composite WWB events with the appropriate frequency, amplitude, and zonal extent, given the evolution of the SST and the warm pool. The WWBs should be stochastic in nature, yet their characteristics should be influenced by the SST. One way of doing this could be to specify the probability distribution function (pdf) of the WWBs be a function of the warm pool extension. The effects of the WWBs on ENSO may therefore be thought of qualitatively as that of multiplicative noise in the sense that their characteristics are influenced by the state of the system, rather than being completely independent external noise.

The above proposed approach to the representation of WWB events in ENSO models that do not actually resolve them requires additional analysis of the observations and, in particular, the use of a model with a shorter time step for a more appropriate representation of the duration of WWBs. We therefore hope to make this the subject of a future work using a hybrid GCM rather than the CZ model.

b. Response to WWBs: Linear or nonlinear?

In view of our results, the issue of whether ENSO responds linearly to WWBs or not becomes somewhat delicate and requires explicit discussion. In our modulated WWB runs, although the ENSO cycle with WWBs was irregular and seemingly chaotic (Fig. 5b), the response of the CZ model to the specified WWB events was, in fact, fairly linear. That is, taking the WWB time series obtained from the modulated WWB run (Fig. 6), filtering out the high-frequency component (up to 3 yr), and then forcing a new experiment with this filtered WWB time series did not significantly affect the slow (2–8 yr) ENSO response (solid line in

Fig. 8). Thus our modulated WWB results, consistent with Roulston and Neelin (2000), imply that ENSO seems to respond mostly linearly to WWB forcing. Only the interannual component of the WWB forcing affects the model ENSO amplitude. [This is in contrast to the stochastic case (dashed line in Fig. 8).]

This paper raises the point, however, that WWB occurrence and characteristics are affected by the SST. We find in our idealized runs that postulating a relation between the large-scale SST field and the statistics of the WWBs has the effect of strengthening the interannual component of the WWBs. This happens because the SST modulation makes the WWBs happen less uniformly in time, shifting WWB power from high frequencies to low frequencies.

This implies that the relation between the WWBs and ENSO may ultimately be nonlinear. The SST modulates the WWBs (a nonlinear effect), and then ENSO responds linearly to the modulated events. This suggests that the WWBs may qualitatively be described as multiplicative rather than additive noise, as mentioned above. Additive stochastic forcing cannot influence the shape of the pdf of a dynamical system. In systems with multiplicative forcing, however, the forcing can modify the shape of the pdf and so fundamentally change the properties of the system response. This is clearly relevant to the role we are promoting for the WWB modulation.

6. Conclusions

We have considered the dynamical consequences of the possibility that the occurrence and characteristics of westerly wind bursts (WWBs) are modulated by the large-scale SST, and therefore by ENSO. This is in contrast to the usual view that WWB events are a stochastic forcing completely external to ENSO and to the coupled equatorial Pacific ocean–atmosphere system. We did so by running the Cane–Zebiak model with two very different idealized representations of WWB events. In one case, the WWBs occur completely deterministically, triggered whenever the warm pool extends eastward beyond some threshold. In the second case, the occurrence of WWB events is purely random and does not depend on the SST. We found that the modulation of the WWBs by the SST made quite a significant difference. When the stochastic WWB events occurred at the same amplitude and average frequency as the modulated ones, the ENSO response was roughly *half as large* as in the case of modulated events. We explained that this occurs because the modulation by the SST imposes an enhanced slow frequency component on the occurrence of WWBs. ENSO responds mostly

linearly to this slow component (cf. Roulston and Neelin 2000). In other words, while a single WWB may not excite an El Niño event, the accumulation of WWBs during a period of increased activity can induce a warming event, and a period of decreased activity can similarly allow a La Niña event. The modulated WWBs occur mainly in bunches prior to and during El Niño events. In the stochastic case, some WWBs occur when the system is ready to enter an El Niño event and during mature events, amplifying ENSO, but WWBs occur with similar probability during La Niña events, which can actually weaken ENSO variability. ENSO is therefore excited much more efficiently by the modulated WWBs than by the purely stochastic WWB events that have less power at slow frequencies. Note that we are proposing that the slow frequency component of the WWB events is created via the modulation by ENSO itself rather than by processes outside the tropical Pacific as suggested by Roulston and Neelin (2000). This modulation of the WWB events by the SST is a nonlinear effect that is somewhat similar to the effect of multiplicative noise in stochastically driven dynamical systems.

We have also shown that including westerly wind bursts modulated by the SST (and hence ENSO) is roughly equivalent to enhancing the ocean–atmosphere coupling coefficient. Both lead ENSO into self-sustained and possibly even chaotic regimes. We speculate that these results may be somewhat relevant to the success of the ENSO hindcasts of Chen et al. (2004), who used the CZ model with no explicit representation of WWBs. According to our results, their model may have roughly compensated for the lack of WWBs by using a stronger ocean–atmosphere coupling strength.

We have considered two extreme idealized cases—purely deterministic WWB events that are completely controlled by the SST and WWBs that are purely stochastic in time—in order to demonstrate the role of WWB modulation. A more realistic scenario most likely lies somewhere in between these two. One expects that the timing and characteristics of WWBs have a random component due to fast weather variability but that the probability distribution function for these variables should depend on the large-scale SST distribution. We discussed this more realistic scenario and outlined a possible approach for a representation of WWBs in hybrid ENSO models that addresses WWB modulation by the SST.

The idealized scenarios examined here demonstrate that treating westerly wind bursts as a purely stochastic forcing misses a very important part of ENSO dynamics. Future studies of the effects of the modulation of

WWB events by ENSO will need to include the many elements neglected here, including a more accurate duration of WWB events; the partially stochastic character of their occurrence, amplitude, and location; their movement with the warm pool edge; and more.

REFERENCES

Barnston, A. G., M. H. Glantz, and Y. X. He, 1999: Predictive skill of statistical and dynamical climate models in SST forecasts during the 1997–98 El Niño episode and the 1998 La Niña onset. *Bull. Amer. Meteor. Soc.,* **80,** 217–243.

Bergman, J. W., and H. H. Hendon, 2000: Cloud radiative forcing of the low-latitude tropospheric circulation: Linear calculations. *J. Atmos. Sci.,* **57,** 2225–2245.

——, ——, and K. M. Weickmann, 2001: Intraseasonal air–sea interactions at the onset of El Niño. *J. Climate,* **14,** 1702–1719.

Blumenthal, M. B., 1991: Predictability of a coupled ocean–atmosphere model. *J. Climate,* **4,** 766–784.

Boulanger, J. P., and Coauthors, 2001: Role of non-linear oceanic processes in the response to westerly wind events: New implications for the 1997 El Niño onset. *Geophys. Res. Lett.,* **28,** 1603–1606.

Cane, M. A., M. Muennich, and S. E. Zebiak, 1990: A study of self-excited oscillations of the tropical ocean–atmosphere system. Part I: Linear analysis. *J. Atmos. Sci.,* **47,** 1562–1577.

Chang, P., B. Wang, T. Li, and L. Ji, 1994: Interactions between the seasonal cycle and the Southern Oscillation—Frequency entrainment and chaos in a coupled ocean-atmosphere model. *Geophys. Res. Lett.,* **21,** 2817–2820.

Chen, D., M. A. Cane, A. Kaplan, S. E. Zebiak, and D. J. Huang, 2004: Predictability of El Niño over the past 148 years. *Nature,* **428,** 733–736.

Chen, S., R. Houze Jr., and B. Mapes, 1996: Multiscale variability of deep convection in relation to large-scale circulation in TOGA COARE. *J. Atmos. Sci.,* **53,** 1380–1409.

Chu, P.-S., 1988: Extratropical forcing and the burst of equatorial westerlies in the western Pacific: A synoptic study. *J. Meteor. Soc. Japan,* **66,** 549–563.

Delcroix, T., G. Eldin, M. McPhaden, and A. Morlière, 1993: Effects of westerly wind bursts upon the western equatorial Pacific Ocean, February–April 1991. *J. Geophys. Res.,* **98** (C9), 16 379–16 385.

Eckert, C., and M. Latif, 1997: Predictability of a stochastically forced hybrid coupled model of El Niño. *J. Climate,* **10,** 1488–1504.

Fan, Y., M. R. Allen, D. L. T. Anderson, and M. A. Balmaseda, 2000: How predictability depends on the nature of uncertainty in initial conditions in a coupled model of ENSO. *J. Climate,* **13,** 3298–3313.

Farrell, B., 1988: Optimal excitation of neutral Rossby waves. *J. Atmos. Sci.,* **45,** 163–172.

Fedorov, A. V., 2002: The response of the coupled tropical ocean–atmosphere to westerly wind bursts. *Quart. J. Roy. Meteor. Soc.,* **128,** 1–23.

——, S. L. Harper, S. G. Philander, B. Winter, and A. Wittenberg, 2003: How predictable is El Niño? *Bull. Amer. Meteor. Soc.,* **84,** 911–919.

Harrison, D. E., and G. A. Vecchi, 1997: Westerly wind events in the tropical Pacific, 1986–95. *J. Climate,* **10,** 3131–3156.

Jin, F.-F., D. Neelin, and M. Ghil, 1994: El Niño on the devil's staircase: Annual subharmonic steps to chaos. *Science,* **264,** 70–72.

Keen, R. A., 1982: The role of cross-equatorial tropical cyclone pairs in the Southern Oscillation. *Mon. Wea. Rev.,* **110,** 1405–1416.

Kerr, R. A., 1999: Atmospheric science: Does a globe-girdling disturbance jigger El Niño? *Science,* **285,** 322–323.

Kessler, W. S., 2001: EOF representations of the Madden–Julian oscillation and its connection with ENSO. *J. Climate,* **14,** 3055–3061.

——, 2002: Is ENSO a cycle or a series of events? *Geophys. Res. Lett.,* **29,** 2125, doi:10.1029/2002GL015924.

——, and R. Kleeman, 2000: Rectification of the Madden–Julian oscillation into the ENSO cycle. *J. Climate,* **13,** 3560–3575.

——, M. J. McPhaden, and K. M. Weickmann, 1995: Forcing of intraseasonal Kelvin waves in the equatorial Pacific. *J. Geophys. Res.,* **100** (C6), 10 613–10 631.

Kleeman, R., and A. M. Moore, 1997: A theory for the limitation of ENSO predictability due to stochastic atmospheric transients. *J. Atmos. Sci.,* **54,** 753–767.

Landsea, C. W., and J. A. Knaff, 2000: How much skill was there in forecasting the very strong 1997–98 El Niño? *Bull. Amer. Meteor. Soc.,* **81,** 2107–2119.

Latif, M., J. Biercamp, and H. von Storch, 1988: The response of a coupled ocean–atmosphere general circulation model to wind bursts. *J. Atmos. Sci.,* **45,** 964–979.

Lengaigne, M., E. Guilyardi, J. P. Boulanger, C. Menkes, P. Delecluse, P. Inness, J. Cole, and J. Slingo, 2004: Triggering of El Niño by westerly wind events in a coupled general circulation model. *Climate Dyn.,* **23,** 601–620.

Luther, D. S., D. E. Harrison, and R. A. Knox, 1983: Zonal winds in the central equatorial Pacific and El Niño. *Science,* **222,** 327–330.

McPhaden, M. J., 1999: Climate oscillations: Genesis and evolution of the 1997–98 El Niño. *Science,* **283,** 950–954.

——, 2004: Evolution of the 2002/03 El Niño. *Bull. Amer. Meteor. Soc.,* **85,** 677–695.

——, H. P. Freitag, S. P. Hayes, B. A. Taft, Z. Chien, and K. Wyrtki, 1988: The response of the equatorial Pacific Ocean to a westerly wind burst in may 1986. *J. Geophys. Res.,* **93** (C9), 10 589–10 603.

——, and Coauthors, 1998: The tropical ocean global atmosphere observing system: A decade of progress. *J. Geophys. Res.,* **103** (C7), 14 169–14 240.

Moore, A. M., and R. Kleeman, 1996: The dynamics of error growth and predictability in a coupled model of ENSO. *Quart. J. Roy. Meteor. Soc.,* **122,** 1405–1446.

——, and ——, 1999: Stochastic forcing of ENSO by the intraseasonal oscillation. *J. Climate,* **12,** 1199–1220.

——, and ——, 2001: The differences between the optimal perturbations of coupled models of ENSO. *J. Climate,* **14,** 138–163.

Penland, C., and P. D. Sardeshmukh, 1995: The optimal growth of tropical sea surface temperature anomalies. *J. Climate,* **8,** 1999–2024.

Perigaud, C. M., and C. Cassou, 2000: Importance of oceanic decadal trends and westerly wind bursts for forecasting El Niño. *Geophys. Res. Lett.,* **27,** 389–392.

Roulston, M. S., and J. D. Neelin, 2000: The response of an ENSO model to climate noise, weather noise and intraseasonal forcing. *Geophys. Res. Lett.,* **27,** 3723–3726.

Thompson, C. J., and D. S. Battisti, 2000: A linear stochastic dynamical model of ENSO. Part I: Model development. *J. Climate,* **13,** 2818–2883.

Tziperman, E., L. Stone, M. A. Cane, and H. Jarosh, 1994: El Niño chaos: Overlapping of resonances between the seasonal cycle and the Pacific Ocean–atmosphere oscillator. *Science,* **264,** 72–74.

——, M. A. Cane, and S. E. Zebiak, 1995: Irregularity and locking to the seasonal cycle in an ENSO prediction model as explained by the quasi-periodicity route to chaos. *J. Atmos. Sci.,* **52,** 293–306.

Vecchi, G., and D. Harrison, 2000: Tropical Pacific sea surface temperature anomalies, El Niño, and equatorial westerly wind events. *J. Climate,* **13,** 1814–1830.

Verbickas, S., 1998: Westerly wind bursts in the tropical Pacific. *Weather,* **53,** 282–284.

Xue, Y., M. A. Cane, and S. E. Zebiak, 1997: Predictability of a coupled model of ENSO using singular vector analysis. Part I: Optimal growth in seasonal background and ENSO cycles. *Mon. Wea. Rev.,* **125,** 2043–2056.

Yu, L., and M. M. Rienecker, 1998: Evidence of an extratropical atmospheric influence during the onset of the 1997–98 El Niño. *Geophys. Res. Lett.,* **25,** 3537–3540.

——, R. A. Weller, and T. W. Liu, 2003: Case analysis of a role of ENSO in regulating the generation of westerly wind bursts in the western equatorial Pacific. *J. Geophys. Res.,* **108,** 3128, doi:10.1029/2002JC001498.

Zavala-Garay, J., C. Zhang, A. Moore, and R. Kleeman, 2005: The linear response of ENSO to the Madden–Julian oscillation. *J. Climate,* **18,** 2441–2459.

Zebiak, S. E., 1989: On the 30–60 day oscillation and the prediction of El Niño. *J. Climate,* **2,** 1381–1387.

——, and M. A. Cane, 1987: A model El Niño–Southern Oscillation. *Mon. Wea. Rev.,* **115,** 2262–2278.

Zhang, C. D., 1996: Atmospheric intraseasonal variability at the surface in the tropical western Pacific Ocean. *J. Atmos. Sci.,* **53,** 739–758.